DALTON
FULL PAPER

The self-exchange of a nonbonding electron *via* the outer-sphere pathway: reorganizational energy and electronic coupling matrix element for the $V(OH_2)_6^{2+/3+}$, $Ru(OH_2)_6^{2+/3+}$, $V(OH_2)_6^{3+/4+}$, and $Ru(OH_2)_6^{3+/4+}$ couples †

François P. Rotzinger

Institut de chimie physique, Ecole Polytechnique Fédérale, CH-1015 Lausanne, Switzerland. E-mail: francois.rotzinger@epfl.ch

Received 21st September 2001, Accepted 6th November 2001
First published as an Advance Article on the web 24th January 2002

The electron self-exchange reaction *via* the outer-sphere pathway of $V(OH_2)_6^{2+/3+}$, $Ru(OH_2)_6^{2+/3+}$, $V(OH_2)_6^{3+/4+}$, and $Ru(OH_2)_6^{3+/4+}$ was investigated with quantum chemical methods. The reorganizational energy (λ) and the nuclear frequency factor (ν_n) were computed on the basis of $M(OH_2)_6{\cdot}(OH_2)_{12}^{n+}$ (M = V, Ru; n = 2, 3, 4) model compounds, in which the 12 water molecules represent the second coordination sphere. The constant for the association of the reactants (K_A) was calculated *via* the Fuoss equation. The electronic coupling matrix element (H_{ab}) was computed on the basis of $[M(OH_2)_6]_2^{n+}$ (M = V, Ru; n = 5, 7) dimers, and the electronic frequency factor (ν_{el}) was determined from H_{ab} and λ. Because, for the present redox couples, ν_n is much greater than ν_{el}, the second-order rate constant (k) is equal to $K_A\nu_{el}e^{-\Delta E^{\ddagger}/RT}$ (whereby $\Delta E^{\ddagger} = \lambda/4$). The *experimental* rate constant for the $V(OH_2)_6^{2+/3+}$ self-exchange reaction is too low because side reactions involving ClO_4^-, the anion of the supporting electrolyte, have not been considered. The present computations suggest a rate constant in the range of 0.14–0.19 M^{-1} s^{-1} (25 °C, I = 2.0 M). The calculated rate constant for the $Ru(OH_2)_6^{2+/3+}$ self-exchange reaction agrees with experiment. For the $V(OH_2)_6^{3+/4+}$ self-exchange reaction, an estimated rate constant of (1–6) × 10^{-6} M^{-1} s^{-1} (25 °C, I = 2.0 M) is predicted. The second-order rate constant for the $Ru(OH_2)_6^{3+/4+}$ self-exchange process is estimated as 0.07 or 18 M^{-1} s^{-1} (25 °C, I = 5.0 M), respectively, for a δ or a σ donor–acceptor interaction, whereby the preferred pathway is yet unknown.

Introduction

Recently, the electron self-exchange reaction of the $Fe(OH_2)_6^{2+/3+}$ couple *via* the outer-sphere pathway [eqn. (1)] has been revisited using quantum chemical methods.[1]

$$\mathbf{Fe}(OH_2)_6^{3+} + Fe(OH_2)_6^{2+} \longrightarrow \mathbf{Fe}(OH_2)_6^{2+} + Fe(OH_2)_6^{3+} \quad (1)$$

In this reaction, an electron of a nonbonding orbital is exchanged. The second-order rate constant (k) was computed on the basis of the theory of Marcus,[2] Hush,[3] Levich *et al.*,[4] and Sutin[5] [eqn. (2)].

$$k = K_A\kappa_{el}\nu_n e^{-\Delta E^{\ddagger}/RT} \quad (2)$$

K_A is the constant for the association of the reactants. It was calculated according to Fuoss [eqns. (3) and (4)],[6] whereby e = 4.80298 × 10^{-10} esu, N_A = 6.0221367 × 10^{23} mol^{-1}, D_s = 78.54 (for water), R = 8.31432 × 10^7 erg (g mol)$^{-1}$ deg^{-1}, T: temperature [K], I: ionic strength [M], r = distance between the two reactants in the transition state [cm], and z_1 and z_2 are the charges of the reactants.

$$K_A = \frac{4\pi N_A r^3}{3000} e^{-w_r/RT} \quad (3)$$

$$w_r = \frac{z_1 z_2 e^2 N_A}{D_S r(1+\kappa r)} \times 10^{-10}\ [\text{kJ mol}^{-1}]$$
$$\kappa = \left(\frac{8\pi N_A{}^2 e^2}{1000 D_S RT}\right)^{1/2} I^{1/2} \quad (4)$$

κ_{el} [eqn. (5)] is the electronic transmission coefficient, ν_{el} [eqn. (6)] and ν_n [eqns. (7) and (8)], respectively, are the electronic and nuclear frequency factors, and H_{ab} is the electronic coupling matrix element.[5,7] $E_i^{\ddagger}$ is the energy change associated with the vibrational mode ν_i to bring the reactants into the transition state. ν_i is the average normal mode i of the $M(OH_2)_6^{2+/3+}$ or $M(OH_2)_6^{3+/4+}$ couples. $\Delta E^{\ddagger}$, the activation energy, is related to the total reorganizational energy λ *via* eqn. (9).

$$\kappa_{el} = \frac{2(1 - e^{-\nu_{el}/2\nu_n})}{2 - e^{-\nu_{el}/2\nu_n}} \quad (5)$$

$$\nu_{el} = gH_{ab}{}^2/\lambda^{1/2},\ g = 1.75 \times 10^{13}\ \text{kJ}^{-3/2}\ \text{s}^{-1} \quad (6)$$

$$\nu_{in+if} = \left(\frac{\sum_i \nu_i{}^2 E_i^{\ddagger}}{\sum_i E_i^{\ddagger}}\right)^{1/2} \quad (7)$$

$$\nu_n = \left(\frac{\nu_{ou}{}^2\lambda_{ou} + \nu_{in+if}{}^2\lambda_{in+if}}{\lambda_{ou} + \lambda_{in+if}}\right)^{1/2} \quad (8)$$

whereby ν_{ou} = 30 cm^{-1} [7]

$$\lambda = 4\Delta E^{\ddagger} \quad (9)$$

† Based on the presentation given at Dalton Discussion No. 4, 10–13th January 2002, Kloster Banz, Germany.

Electronic supplementary information (ESI) available: Tables of atomic coordinates. See http://www.rsc.org/suppdata/dt/b1/b108627h/

ν_{in+if} is the nuclear frequency factor that arises from the inner shell and interfacial vibrational modes, and λ_{in+if} ($= \lambda_{in} + \lambda_{if}$) is the sum of the inner shell and interfacial reorganization energies (*vide infra*). ν_{ou} is the mode for the reorganization of the bulk solvent, and λ_{ou} is the solvent reorganization energy, that was calculated classically[5] (*vide infra*). The parameters ν_i, $E_i^{\ddagger}$, λ_{in+if}, λ, and $\Delta E^{\ddagger}$ were computed quantum chemically on the basis of $M(OH_2)_6 \cdot (OH_2)_{12}^{n+}$ (M = V, Ru; n = 2, 3, or 4) model compounds, in which $(OH_2)_{12}$ represents the second coordination sphere. H_{ab} was calculated quantum chemically at various M ⋯ M distances (r) of $[M(OH_2)_6]_2^{n+}$ dimers (M = V, Ru; n = 5 or 7), in which the second coordination sphere was not included.[1]

The important findings from the study[1] of reaction (1) are: (i) the Fe ⋯ Fe separation in the transition state is ≈6.3 Å. This distance corresponds approximately to the close contact of the $Fe(OH_2)_6^{2+}$ and $Fe(OH_2)_6^{3+}$ reactants, whereby there is no interpenetration of the ligand spheres. (ii) The electronic coupling matrix element (H_{ab}) decreases with increasing Fe ⋯ Fe distance (in the range of 4.5–9.5 Å). (iii) The face-to-face approach of the reactants is sterically most favorable. It yields the strongest donor–acceptor interaction and therefore, the largest H_{ab} at a given Fe ⋯ Fe distance. (iv) ν_n is much larger than ν_{el}: thus, k is independent of ν_n and can be expressed *via* eqn. (10).

$$k = K_A \nu_{el} e^{-\Delta E^{\ddagger}/RT} \tag{10}$$

(v) The total reorganizational energy λ is not just the sum of the inner shell (λ_{in}) and the outer-sphere (λ_{ou}) terms [eqn. (11)];

$$\lambda = \lambda_{in} + \lambda_{ou} \tag{11}$$

the reorganization of the interfacial H-bonds between the first and second coordination spheres (λ_{if}) has to be included.

Thus, the reorganizational energy of $M(OH_2)_6^{2+/3+}$ couples, for example, has to be computed using eqn. (12) instead of eqn. (11).

$$\lambda = \lambda_{in} + \lambda_{if} + \lambda_{ou} \tag{12}$$

The present study reports on the electron self-exchange reaction of the $V(OH_2)_6^{2+/3+}$ and $Ru(OH_2)_6^{2+/3+}$ couples *via* the outer-sphere pathway. In these two reactions, a nonbonding electron is exchanged as in the $Fe(OH_2)_6^{2+/3+}$ couple. Furthermore, the model has been applied to the $V(OH_2)_6^{3+/4+}$ and $Ru(OH_2)_6^{3+/4+}$ couples, in which also a nonbonding electron is exchanged. For these latter two couples, no experimental data is available. Thus, the computed data might be useful for the discussion of redox reactions involving these couples in strongly acidic aqueous solution and for the comparison with the more favorable pathway that proceeds *via* the hydroxo complexes, the $VOH(OH_2)_5^{2+/3+}$ and $RuOH(OH_2)_5^{2+/3+}$ couples.

It is striking that the measured[8–11] self-exchange rates of the $M(OH_2)_6^{2+/3+}$ (M = V, Fe, and Ru) couples vary by a factor of more than 1000, although in all of these reactions a nonbonding electron is exchanged. The present computations indicate that the measured[9] rate constant of 0.010 M^{-1} s^{-1} for the $V(OH_2)_6^{2+/3+}$ electron self-exchange reaction is too low because side reactions involving the supporting electrolyte, the perchlorate anion, were not taken into account: this anion oxidizes $V(OH_2)_6^{2+}$ quite rapidly.[12] The present calculations suggest a second-order rate constant in the range of 0.14–0.19 M^{-1} s^{-1} (25 °C and I = 2.0). The origin of the different reactivities of the $V(OH_2)_6^{2+/3+}$, $Fe(OH_2)_6^{2+/3+}$, and $Ru(OH_2)_6^{2+/3+}$ couples is analyzed.

Computational details

All of the calculations have been performed on HP 9000/C200 and HP 9000/735 computers using the GAMESS[13] programs.

The calculations were performed as described[1] for the $Fe^{II/III}$ couple. The reorganizational energy (λ_{fs}) was computed on the basis of $M(OH_2)_6 \cdot (OH_2)_{12}^{2+/3+/4+}$ (M = V, Ru) model species exhibiting D_2 or T symmetry, with all of their computed vibrational frequencies being real. The basis sets of Stevens, Krauss, Basch, and Jasien[14] were used for vanadium and ruthenium, where the inner shells are represented by relativistic effective core potentials, the s and p semi-cores and the s and p valence shells have double-ζ quality, and the valence d shell has triple-ζ quality. The 6–31G basis set[15,16] was used for O and H of water in the first coordination sphere. For water in the second coordination sphere, the basis sets 6–31G and STO–4G,[17] respectively, were taken for O and H. The geometries were optimized at the Hartree–Fock level for the free ions in the gas phase, and the atomic coordinates are given in Tables S1–S6 (ESI). The total energy (Table 1) was computed by taking into account hydration by the third and further coordination spheres using the polarizable continuum model (PCM).[21–23] Static and dynamic electron correlation were included using the "multiconfigurational self-consistent field second-order quasidegenerate perturbation" (MCQDPT2) method[24,25] as described.[1,26]

The electronic coupling matrix element (H_{ab}) was calculated at the MCQDPT2 level on the basis of $[M(OH_2)_6]_2^{n+}$ (M = V, Ru; n = 5, 7) species, whose geometries were optimized in S_6 symmetry at the Hartree–Fock level for the free ions in the gas phase. These calculations were performed for various M ⋯ M distances (r) that were kept fixed, otherwise the dimers would dissociate due to the electrostatic repulsion. For the water ligands, the 6–31G basis set was used. The atomic coordinates are given in Tables S7–S10 (ESI). Hydration was not included in the computation of H_{ab}; it cancels out because the PCM solvation energy is equal for the ground and the excited states. In the $[V(OH_2)_6]_2^{7+}$ and $[Ru(OH_2)_6]_2^{5+/7+}$ dimers, there was appreciable static electron correlation; the occupations of the natural orbitals of the complete active space self-consistent field (CAS-SCF) wave function were <1.98 and >0.02 electrons. In this case, the MCQDPT2 method was applied. In the $[V(OH_2)_6]_2^{5+}$ dimer, however, some orbital occupations were 0.993 and 0.007. Thus, the multireference second-order Møller–Plesset (MRMP2) calculations were performed on the basis of the complete active space configuration interaction (CAS-CI) reference wavefunction that was based on the Hartree–Fock (HF) molecular orbitals.[27] The MRMP2 energies of the ^4A_g and ^4A_u states of $[M(OH_2)_6]_2^{7+}$ (M = V, Ru) were computed on the basis of a CAS-CI reference wavefunction with the MOs from a CAS-SCF calculation having a smaller active space. The pertinent data is given in Table 2. The energy difference between the ground and the appropriate excited state is equal to $2H_{ab}$.

Hydration and electron correlation were neglected in the geometry optimizations. These effects were included in the computations of the total energies, for which, however, the zero point energies (ZPE) are not available because the $[M(OH_2)_6 \cdot (OH_2)_{12}^{n+}]^*$ species [see "Results—Reorganizational energy (λ)" section] are not in local minima by definition. Thus, it does not make sense to compute their harmonic vibrational frequencies. Due to the unavailability of these ZPEs, the reorganizational entropy had to be neglected as well.

Results

In this section, it is explained how all of the quantum chemically computed data, that is needed for the determination of k, was obtained. These calculated parameters are the reorganizational energy (λ), the electronic coupling matrix element (H_{ab}), and the nuclear frequency factor (ν_n). As already mentioned in the Introduction, the constant for the association of the reactants was calculated classically *via* eqns. (3) and (4). In the last chapter, the M ⋯ M distance dependence of the

Table 1 Experimental and calculated M–O (M = V, Ru) bond lengths and calculated total energies[a]

Species	Electronic state	Symmetry	*d*(M–O)/Å		Geometry	Total energy[b] (E_1, E_2, E_1* or E_2*)
			Calculated	Experimental		
$V(OH_2)_6{\cdot}(OH_2)_{12}^{2+}$	^4A	T	2.185	2.128[c]	$V(OH_2)_6{\cdot}(OH_2)_{12}^{2+}$	−1441.057203(1)
$V(OH_2)_6^{2+}$	^4A	T			$\mathbf{V(OH_2)}_6{\cdot}(OH_2)_{12}^{2+}$	−527.264582(1)
$[V(OH_2)_6{\cdot}(OH_2)_{12}^{2+}]$*	^4A	D_2			$V(OH_2)_6{\cdot}(OH_2)_{12}^{3+}$	−1441.039087(1)
$[V(OH_2)_6^{2+}]$*	^4A	D_2			$\mathbf{V(OH_2)}_6{\cdot}(OH_2)_{12}^{3+}$	−527.244854(1)
$V(OH_2)_6{\cdot}(OH_2)_{12}^{3+}$	$^3B_2$	D_2	2.016, 2.071, 2.048	1.992[d]	$V(OH_2)_6{\cdot}(OH_2)_{12}^{3+}$	−1440.945908(6)
$V(OH_2)_6^{3+}$	$^3B_2$	D_2			$\mathbf{V(OH_2)}_6{\cdot}(OH_2)_{12}^{3+}$	−526.719870(2)
$[V(OH_2)_6{\cdot}(OH_2)_{12}^{3+}]$*	^3T	T			$V(OH_2)_6{\cdot}(OH_2)_{12}^{2+}$	−1440.891721(10)
$[V(OH_2)_6{\cdot}(OH_2)_{12}^{3+}]$*	$^3B_2$	D_2			$V(OH_2)_6{\cdot}(OH_2)_{12}^{4+}$	−1440.919016(6)
$[V(OH_2)_6^{3+}]$*	^3T	T			$\mathbf{V(OH_2)}_6{\cdot}(OH_2)_{12}^{2+}$	−526.699852(10)
$[V(OH_2)_6^{3+}]$*	$^3B_2$	D_2			$\mathbf{V(OH_2)}_6{\cdot}(OH_2)_{12}^{4+}$	−526.680817(2)
$V(OH_2)_6{\cdot}(OH_2)_{12}^{4+}$	$^2B_3$	D_2	1.861, 1.958, 2.015		$V(OH_2)_6{\cdot}(OH_2)_{12}^{4+}$	−1440.723877(784)
$V(OH_2)_6^{4+}$	$^2B_1$	D_2			$\mathbf{V(OH_2)}_6{\cdot}(OH_2)_{12}^{4+}$	−525.847050(188)
$[V(OH_2)_6{\cdot}(OH_2)_{12}^{4+}]$*	$^2B_3$	D_2			$V(OH_2)_6{\cdot}(OH_2)_{12}^{3+}$	−1440.663544(784)
$[V(OH_2)_6^{4+}]$*	$^2B_1$	D_2			$\mathbf{V(OH_2)}_6{\cdot}(OH_2)_{12}^{3+}$	−525.851762(188)
$Ru(OH_2)_6{\cdot}(OH_2)_{12}^{2+}$	^1A	T	2.188	2.122[e]	$Ru(OH_2)_6{\cdot}(OH_2)_{12}^{2+}$	−1463.433768(50)
$Ru(OH_2)_6^{2+}$	^1A	T			$\mathbf{Ru(OH_2)}_6{\cdot}(OH_2)_{12}^{2+}$	−549.631566(17)
$[Ru(OH_2)_6{\cdot}(OH_2)_{12}^{2+}]$*	^1A	D_2			$Ru(OH_2)_6{\cdot}(OH_2)_{12}^{3+}$	−1463.419990(50)
$[Ru(OH_2)_6^{2+}]$*	^1A	D_2			$\mathbf{Ru(OH_2)}_6{\cdot}(OH_2)_{12}^{3+}$	−549.616998(17)
$Ru(OH_2)_6{\cdot}(OH_2)_{12}^{3+}$	$^2B_2$	D_2	2.052, 2.109, 2.083	2.029[e]	$Ru(OH_2)_6{\cdot}(OH_2)_{12}^{3+}$	−1463.294920(20)
$Ru(OH_2)_6^{3+}$	$^2B_2$	D_2			$\mathbf{Ru(OH_2)}_6{\cdot}(OH_2)_{12}^{3+}$	−549.066381(5)
$[Ru(OH_2)_6{\cdot}(OH_2)_{12}^{3+}]$*	^2T	T			$Ru(OH_2)_6{\cdot}(OH_2)_{12}^{2+}$	−1463.253750(75)
$[Ru(OH_2)_6{\cdot}(OH_2)_{12}^{3+}]$*	$^2B_2$	D_2			$Ru(OH_2)_6{\cdot}(OH_2)_{12}^{4+}$	−1463.281903(20)
$[Ru(OH_2)_6^{3+}]$*	^2T	T			$\mathbf{Ru(OH_2)}_6{\cdot}(OH_2)_{12}^{2+}$	−549.053990(75)
$[Ru(OH_2)_6^{3+}]$*	$^2B_2$	D_2			$\mathbf{Ru(OH_2)}_6{\cdot}(OH_2)_{12}^{4+}$	−549.051346(5)
$Ru(OH_2)_6{\cdot}(OH_2)_{12}^{4+}$	$^3B_3$	D_2	1.957, 2.023, 2.053		$Ru(OH_2)_6{\cdot}(OH_2)_{12}^{4+}$	−1463.076743(588)
$Ru(OH_2)_6^{4+}$	$^3B_3$	D_2			$\mathbf{Ru(OH_2)}_6{\cdot}(OH_2)_{12}^{4+}$	−548.224373(149)
$[Ru(OH_2)_6{\cdot}(OH_2)_{12}^{4+}]$*	$^3B_3$	D_2			$Ru(OH_2)_6{\cdot}(OH_2)_{12}^{3+}$	−1463.035002(588)
$[Ru(OH_2)_6^{4+}]$*	$^3B_1$	D_2			$\mathbf{Ru(OH_2)}_6{\cdot}(OH_2)_{12}^{3+}$	−548.227032(149)

[a] Units: hartrees. [b] In parentheses: number of configuration state functions of the CAS-SCF wavefunction. [c] Average *d*(V^{II}–O), ref. 18. [d] Average *d*(V^{III}–O), ref. 19. [e] Ref. 20.

Table 2 Electronic coupling matrix element (H_{ab}) and total MCQDPT2 energies of the pertinent states of $[M(OH_2)_6]_2^{n+}$ (M = V, Ru; n = 5, 7)

Redox couple	*r*/Å	*E*/hartrees		No. of CSFs[a]	H_{ab}/kJ mol^{-1}
		Ground state	Excited state		
$V^{II/III}$	9.451	−1053.683290	−1053.683288	126	0.003[b]
$V^{II/III}$	7.948	−1053.634237	−1053.634213	126	0.032
$V^{II/III}$	7.50	−1053.617573	−1053.617526	126	0.062
$V^{II/III}$	6.959	−1053.596044	−1053.595964	126	0.105
$V^{II/III}$	6.50	−1053.576620	−1053.576526	126	0.123
$V^{II/III}$	6.30	−1053.567868	−1053.567769	126	0.130
$V^{II/III}$	6.00	−1053.554394	−1053.554276	126	0.155
$Ru^{II/III}$	9.457	−1098.404283	−1098.404280	13860	0.004
$Ru^{II/III}$	7.888	−1098.354119	−1098.354088	13860	0.041
$Ru^{II/III}$	6.996	−1098.320636	−1098.320547	13860	0.117
$Ru^{II/III}$	6.80	−1098.312813	−1098.312715	13860	0.129
$Ru^{II/III}$	6.50	−1098.300490	−1098.300400	13860	0.118
$Ru^{II/III}$	6.00	−1098.279206	−1098.279141	13860	0.085
$V^{III/IV}$	6.50	−1051.737500[c]	−1051.737495[d]	2	0.007
$V^{III/IV}$	6.50	−1051.723278[e]	−1051.723199[f]	19	0.104
$V^{III/IV}$	6.30	−1051.718443[c]	−1051.718433[d]	2	0.013
$V^{III/IV}$	6.00	−1051.688633[c]	−1051.688614[d]	2	0.025
$Ru^{III/IV}$	7.90	−1096.600476[f]	−1096.600419[e]	9900	0.075
$Ru^{III/IV}$	7.90	−1096.594620[c]	−1096.594617[d]	3	0.004
$Ru^{III/IV}$	7.20	−1096.544073[f]	−1096.543947[e]	9900	0.165
$Ru^{III/IV}$	7.20	−1096.540433[c]	−1096.540425[d]	3	0.011
$Ru^{III/IV}$	6.80	−1096.509245[f]	−1096.509096[e]	9900	0.196
$Ru^{III/IV}$	6.80	−1096.506456[c]	−1096.506449[d]	3	0.009
$Ru^{III/IV}$	6.50	−1096.481803[f]	−1096.481664[e]	9900	0.182
$Ru^{III/IV}$	6.50	−1096.479783[c]	−1096.479775[d]	3	0.011
$Ru^{III/IV}$	6.00	−1096.433565[f]	−1096.433453[e]	9900	0.147
$Ru^{III/IV}$	6.00	−1096.432663[c]	−1096.432655[d]	3	0.011

[a] CSFs: configuration state functions of the CAS-SCF or CAS-CI reference wavefunction. The MCQDPT2 computations were performed in C_i symmetry. [b] The numerical precision in the total energies is about 1×10^{-6} hartrees. Thus, the error in H_{ab} is ±0.003 kJ mol^{-1}. [c] ^4E_u state. [d] ^4E_g state. [e] ^4A_g state. [f] ^4A_u state.

Table 3 Reorganizational energy and its components[a]

Redox couple	λ_{in} [eqn. (18)]	λ_{fs} [eqn. (14)]	λ_{if} [eqn. (16)]	λ_{ou}' [eqn. (15)]	λ_{ou} [eqn. (17)]	λ [eqn. (13)]	r/Å
$V^{II/III}$	104.4	189.8	28.3	39.8	96.9	229.6	6.30
			28.3	43.5	100.6	233.3	6.50
$Ru^{II/III}$	70.8	144.3	17.5	43.4	99.4	187.7	6.50
$Fe^{II/III}$ [b]	81.9	162.8	22.9	40.4	98.4	203.2	6.30
$V^{III/IV}$	90.2	229.0	79.7	40.6	99.7	269.6	6.30
			79.7	44.3	103.4	273.3	6.50
$Ru^{III/IV}$	32.5	143.8	53.8	43.9	101.4	187.7	6.50
			53.8	49.0	106.5	192.8	6.80

[a] Units: kJ mol^{-1}. [b] Ref. 1.

second-order rate constants (k), calculated according to eqn. (10), is analyzed.

Reorganizational energy (λ)

λ was computed on the basis of eqn. (13)[1] because it cannot be evaluated *via* eqn. (12) in a straightforward manner.

$$\lambda = \lambda_{fs} + \lambda_{ou}' \qquad (13)$$

λ_{fs} (Table 3) is the reorganizational energy of the hexaaqua ion including its second coordination sphere (Figs. 1 and 2),

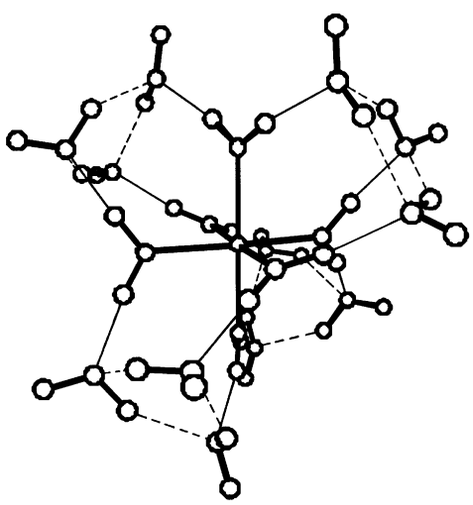

Fig. 1 Perspective view of the $V(OH_2)_6\cdot(OH_2)_{12}^{3+}$ ion exhibiting D_2 symmetry. The dashed lines represent the hydrogen bonds within the cyclic water trimers in the second coordination sphere.

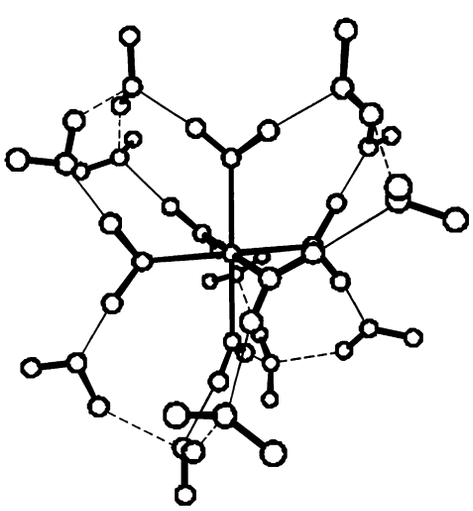

Fig. 2 Perspective view of the $V(OH_2)_6\cdot(OH_2)_{12}^{4+}$ ion exhibiting D_2 symmetry. The dashed lines represent the hydrogen bonds within the water trimers in the second coordination sphere.

whereby the latter was represented by $12H_2O$ molecules.[1] λ_{fs} was calculated *via* eqn. (14) on the basis of $M(OH_2)_6\cdot(OH_2)_{12}^{n+}$ (M = V, Ru; n = 2, 3 or 4) model compounds.

$$\lambda_{fs} = E_{1,fs}^* + E_{2,fs}^* - (E_{1,fs} + E_{2,fs}) \qquad (14)$$

$E_{1,fs}$ and $E_{2,fs}$ are the total energies of the two reactants, the reductant and the oxidant, respectively, in their stable geometries. $E_{1,fs}^*$ is the energy of the reductant at the geometry of the oxidant and likewise, $E_{2,fs}^*$ is the energy of the oxidant at the geometry of the reductant. For a $M(OH_2)_6^{2+/3+}$ self-exchange reaction for example, $E_{1,fs}$, $E_{2,fs}$, $E_{1,fs}^*$, and $E_{2,fs}^*$ correspond to the total energies of $M(OH_2)_6\cdot(OH_2)_{12}^{2+}$, $M(OH_2)_6\cdot(OH_2)_{12}^{3+}$, $[M(OH_2)_6\cdot(OH_2)_{12}^{2+}]^*$, and $[M(OH_2)_6\cdot(OH_2)_{12}^{3+}]^*$, whereby $[M(OH_2)_6\cdot(OH_2)_{12}^{n+}]^*$ represents a reactant at the geometry of its redox partner. λ_{fs} is the energy for the electron transfer *at frozen nuclei* and arises from a *vertical* electron transition. All of the $E_{1,fs}$, $E_{2,fs}$, $E_{1,fs}^*$, and $E_{2,fs}^*$ energies (Table 1) were computed by taking into account hydration using the polarizable continuum model (PCM).[21–23] Static and dynamic electron correlation were calculated *via* the "multiconfigurational self-consistent field second-order quasidegenerate perturbation" (MCQDPT2) method.[24–26]

The computation of λ_{fs} required the geometry optimizations of $M(OH_2)_6\cdot(OH_2)_{12}^{n+}$ (M = V, Ru; n = 2, 3, 4). The structures of the $M(OH_2)_6\cdot(OH_2)_{12}^{2+}$ and $M(OH_2)_6\cdot(OH_2)_{12}^{3+}$ ions (M = V, Ru), respectively, resemble those of Fe^{II} or Fe^{III}.[1] The $12H_2O$ molecules in the second coordination sphere form 4 cyclic trimers. As an example, the structure of $V(OH_2)_6\cdot(OH_2)_{12}^{3+}$ is shown in Fig. 1.

The structures of the $M(OH_2)_6\cdot(OH_2)_{12}^{4+}$ ions (Fig. 2) are different: two *trans* M–O bonds are quite short, 1.861 and 1.957 Å for V^{IV} and Ru^{IV}, respectively (Table 4). These water molecules are very acidic because their O–H bonds are unusually long, 1.055 and 1.038 Å for V^{IV} and Ru^{IV}. The O–H bonds of the other water ligands are shorter than 1.00 Å, and those in the $M(OH_2)_6\cdot(OH_2)_{12}^{3+}$ and $M(OH_2)_6\cdot(OH_2)_{12}^{2+}$ ions, respectively, are shorter than 0.98 and 0.96 Å. The H-bonds of the acidic protons to water in the second coordination sphere are also quite short, 1.388 and 1.422 Å for V^{IV} and Ru^{IV}, respectively, such that one H-bond of each cyclic trimer is broken. Thus, in the 4+ ions, the 12 water molecules in the second coordination sphere form 4 open trimers.

λ_{ou}' is the reorganizational energy of the solvent starting from the third coordination sphere. It was calculated according to eqn. (15).[5]

$$\lambda_{ou}' = 753.12\left[\frac{1}{2}\left(\frac{1}{r_1'} + \frac{1}{r_2'}\right) - \frac{1}{r}\right] [\text{kJ mol}^{-1}] \qquad (15)$$

The radii of the two reactants including their second coordination spheres, r_1' and r_2' (Table 5), were determined from the PCM cavity volumes as described elsewhere.[1] r is the separation of the two metals in the transition state. The reorganizational energy of the H-bonds between the second

Table 4 Selected internal coordinates of the $M(OH_2)_6\cdot(OH_2)_{12}^{n+}$ ions (M = V, Ru; n = 2, 3, 4)

	d(M–O)/Å	d(H ⋯ O)$_{1-2}$/Å	d(O–H)$_1$/Å	d(O–H)$_2$/Å
$V(OH_2)_6\cdot(OH_2)_{12}^{2+}$	2.185	1.863 [a]	0.959 [b]	0.988, 0.975 [c] Average: 0.982
$V(OH_2)_6\cdot(OH_2)_{12}^{3+}$	2.016, 2.071, 2.048 [d] Average: 2.045	1.710, 1.749, 1.726 [e] Average: 1.728	0.976, 0.971, 0.974 [f] Average: 0.974	0.987, 0.980, 0.986, 0.980, 0.986, 0.980 [f] Average: 0.983
$V(OH_2)_6\cdot(OH_2)_{12}^{4+}$	1.861, 1.956, 2.015 [d] Average: 1.944	1.388, 1.617, 1.791 [e] Average: 1.599	1.055, 0.994, 0.977 [f] Average: 1.009	0.983, 0.980, 0.989, 0.984, 0.987, 0.988 [f] Average: 0.985
$Ru(OH_2)_6\cdot(OH_2)_{12}^{2+}$	2.188	1.853 [a]	0.958 [b]	0.988, 0.976 [c] Average: 0.982
$Ru(OH_2)_6\cdot(OH_2)_{12}^{3+}$	2.052, 2.109, 2.083 [d] Average: 2.081	1.707, 1.745, 1.720 [e] Average: 1.724	0.975, 0.969, 0.973 [f] Average: 0.972	0.987, 0.980, 0.986, 0.980, 0.986, 0.980 [f] Average: 0.983
$Ru(OH_2)_6\cdot(OH_2)_{12}^{4+}$	1.957, 2.023, 2.053 [d] Average: 2.011	1.422, 1.602, 1.772 [e] Average: 1.599	1.038, 0.994, 0.979 [f] Average: 1.004	0.981, 0.980, 0.988, 0.984, 0.988, 0.988 [f] Average: 0.985

[a] 12 equal (H ⋯ O)$_{1-2}$. [b] 12 equal (O–H)$_1$. [c] Two sets of 12 equal (O–H)$_2$. [d] Three sets of 2 equal M–O. [e] Three sets of 4 equal (H ⋯ O)$_{1-2}$. [f] Three sets of 4 equal (O–H)$_1$ or (O–H)$_2$.

Table 5 Radii of the pertinent transition metal hexaaqua ions

			r_{PCM} [a]/Å	
Species	Symmetry	V_{PCM}/Å^3	r_1' or r_2'	r_1 or r_2
$V(OH_2)_6\cdot(OH_2)_{12}^{2+}$	T	449.134	4.751	
$V(OH_2)_6\cdot(OH_2)_{12}^{3+}$	D_2	434.927	4.700	
$V(OH_2)_6\cdot(OH_2)_{12}^{4+}$	D_2	436.127	4.704	
$V(OH_2)_6^{2+}$ [b]	T	182.947		3.522
$V(OH_2)_6^{3+}$ [c]	D_2	170.006		3.437
$V(OH_2)_6^{4+}$ [d]	D_2	169.391		3.432
$Ru(OH_2)_6\cdot(OH_2)_{12}^{2+}$	T	449.003	4.750	
$Ru(OH_2)_6\cdot(OH_2)_{12}^{3+}$	D_2	436.886	4.707	
$Ru(OH_2)_6\cdot(OH_2)_{12}^{4+}$	D_2	441.030	4.722	
$Ru(OH_2)_6^{2+}$ [b]	T	182.938		3.522
$Ru(OH_2)_6^{3+}$ [c]	D_2	175.693		3.474
$Ru(OH_2)_6^{4+}$ [d]	D_2	173.407		3.459

[a] $r_{PCM} = (3/4\pi V_{PCM})^{1/3}$. [b] Second coordination sphere in $M(OH_2)_6\cdot(OH_2)_{12}^{2+}$ omitted. [c] Second coordination sphere in $M(OH_2)_6\cdot(OH_2)_{12}^{3+}$ omitted. [d] Second coordination sphere in $M(OH_2)_6\cdot(OH_2)_{12}^{4+}$ omitted.

and third coordination spheres is neglected in eqn. (13). The validity of this approximation has been established for the $Fe(OH_2)_6^{2+/3+}$ couple.[1]

The interfacial reorganizational energy, λ_{if} [eqn. (16)], was calculated by combining eqns. (12) and (13).[1]

λ_{ou} [eqns. (12) and (16)] is the reorganizational energy of

$$\lambda_{if} = \lambda_{fs} + \lambda_{ou}' - (\lambda_{in} + \lambda_{ou}) \qquad (16)$$

the solvent starting from the second coordination sphere. It was determined classically [5] [eqn. (17)] as λ_{ou}'.

$$\lambda_{ou} = 753.12\left[\frac{1}{2}\left(\frac{1}{r_1}+\frac{1}{r_2}\right)-\frac{1}{r}\right][\text{kJ mol}^{-1}] \qquad (17)$$

r_1 and r_2 (Table 5) are the radii of the hexaaqua ions without second coordination spheres, and r is [as in eqn. (15)] the metal–metal distance in the transition state.

λ_{in} (Table 3) is the inner shell reorganizational energy. It was calculated, similarly as λ_{fs}, *via* eqn. (18).

$$\lambda_{in} = E_{1,in}^* + E_{2,in}^* - (E_{1,in} + E_{2,in}) \qquad (18)$$

$E_{1,in}$ and $E_{2,in}$ are the total energies of the $M(OH_2)_6^{n+}$ (M = V, Ru; n = 2, 3, 4) fragments of $M(OH_2)_6\cdot(OH_2)_{12}^{n+}$ (where the $12H_2O$s of the second coordination sphere were omitted), and $E_{1,in}^*$ and $E_{2,in}^*$ are the energies of these reactants at the geometries of their respective redox partners (Table 1). All of these

Table 6 Classically calculated terms [a]

Redox couple	r [b]/Å	λ_{ou}	λ_{ou}'	w_r	K_A/M^{-1}
$V^{II/III}$	9.451	136.8	79.7	2.1 [c]	0.92
$V^{II/III}$	7.948	121.7	64.6	2.8 [c]	0.40
$V^{II/III}$	7.50	116.1	59.0	3.2 [c]	0.298
$V^{II/III}$	6.959	108.3	51.2	3.6 [c]	0.199
$V^{II/III}$	6.50	100.6	43.5	4.1 [c]	0.135
$V^{II/III}$	6.30	96.9	39.8	4.3 [c]	0.112
$V^{II/III}$	6.00	91.0	33.9	4.7 [c]	0.083
$V^{III/IV}$	6.50	103.4	44.3	8.1 [c]	0.026
$V^{III/IV}$	6.30	99.7	40.6	8.6 [c]	0.020
$V^{III/IV}$	6.00	93.8	34.7	9.3 [c]	0.013
$Ru^{II/III}$	9.457	135.7	79.6	1.4 [d]	1.21
$Ru^{II/III}$	7.888	119.8	63.8	2.0 [d]	0.56
$Ru^{II/III}$	6.996	107.7	51.6	2.5 [d]	0.319
$Ru^{II/III}$	6.80	104.6	48.5	2.6 [d]	0.278
$Ru^{II/III}$	6.50	99.4	43.4	2.8 [d]	0.222
$Ru^{II/III}$	6.00	89.8	33.8	3.3 [d]	0.146
$Ru^{III/IV}$	7.90	121.9	64.4	3.9 [d]	0.253
$Ru^{III/IV}$	7.20	112.7	55.1	4.7 [d]	0.142
$Ru^{III/IV}$	6.80	106.5	49.0	5.2 [d]	0.097
$Ru^{III/IV}$	6.50	101.4	43.9	5.7 [d]	0.071
$Ru^{III/IV}$	6.00	91.7	34.2	6.5 [d]	0.039

[a] Units: kJ mol^{-1}. [b] r is the M ⋯ M distance. [c] At 25 °C, I = 2.0 M. [d] At 25 °C, I = 5.0 M.

inner shell reorganizational energies were computed by taking into account electron correlation, but not hydration. The second coordination sphere, described by $12H_2O$s, has to be removed for the computation of λ_{in} that is due to the reorganization of the free $M(OH_2)_6^{2+/3+}$ or $M(OH_2)_6^{3+/4+}$ couple. Thus, it does not make sense to treat hydration starting from the second coordination sphere using a continuum model.

λ_{fs} and λ_{in} (Table 3) are independent of r, but λ_{ou} and λ_{ou}' (Table 6) depend on the M ⋯ M distance (r). λ_{if} is almost independent of r because the distance dependence of λ_{ou} and λ_{ou}' cancels in the difference $\lambda_{ou}' - \lambda_{ou}$ [eqn. (16)]. λ [eqn. (13)] depends on r. At a given M ⋯ M distance, λ_{ou} and λ_{ou}' neither depend on the charges of the reactants nor on the nature of the metal. In contrast, λ_{fs} and λ_{in} depend on the metal. They are different for the $V(OH_2)_6^{2+/3+}$, $Fe(OH_2)_6^{2+/3+}$, and $Ru(OH_2)_6^{2+/3+}$ couples, although in all of these cases, the charge is equal, and a nonbonding electron is exchanged. For the $M(OH_2)_6^{3+/4+}$ (M = V, Ru) couples, λ_{in} has to be taken with care because the second coordination sphere is bound very strongly to the first one (*vide supra*). Furthermore, the third coordination sphere might also be bound quite strongly to the second coordination sphere. Thus, λ might be larger because the reorganizational energy of

the interface between the second and third coordination spheres might not be negligible as in the $M(OH_2)_6^{2+/3+}$ couples. λ_{fs} is quite different for the two $V(OH_2)_6^{3+/4+}$ and $Ru(OH_2)_6^{3+/4+}$ couples (Table 3).

Because experimental self-exchange rates are not available for the $V(OH_2)_6^{3+/4+}$ and $Ru(OH_2)_6^{3+/4+}$ couples, the distance dependence of λ_{ou}', λ_{ou}, and also H_{ab}, was not investigated over a wide range of r. These energies were computed for the most likely interval of M ⋯ M separations.

Electronic coupling matrix element (H_{ab})

It arises from the interaction of the donor and the acceptor orbitals in the transition state that was modeled by $[M(OH_2)_6]_2^{n+}$ (M = V, Ru; n = 5, 7) dimers (Fig. 3). As in reaction

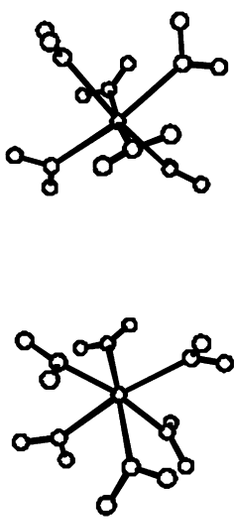

Fig. 3 Perspective view of the $[Ru(OH_2)_6]_2^{5+}$ dimer with S_6 symmetry (the Ru ⋯ Ru distance is 6.80 Å).

(1), a nonbonding electron is exchanged in the $V(OH_2)_6^{2+/3+}$, $Ru(OH_2)_6^{2+/3+}$, $V(OH_2)_6^{3+/4+}$, and $Ru(OH_2)_6^{3+/4+}$ couples. The sterically most favorable arrangement of the reactants was found for the face-to-face approach (Fig. 3).[1] In the $[M(OH_2)_6]_2^{n+}$ dimers (Fig. 3) with S_6 symmetry, the two $M(OH_2)_6$ fragments have C_3 symmetry, and the valence d orbitals split as shown in Fig. 4. The d_π levels are nonbonding and correspond to the t_{2g}

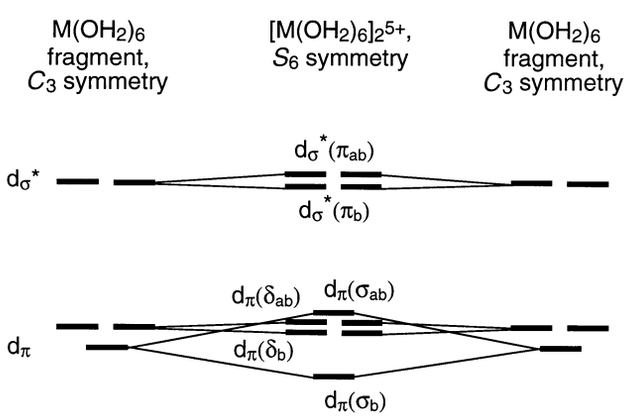

Fig. 4 Qualitative molecular orbital diagram for $[M(OH_2)_6]^{n+}$ dimers.

orbitals in O_h symmetry. For each $M(OH_2)_6$ fragment, two of the three d_π levels are degenerate. The antibonding d_σ* levels (the e_g* levels in O_h symmetry) are also doubly degenerate.

The two non-degenerate d_π molecular orbitals (MOs) lie in the M ⋯ M axis and have each the shape of a d_{z^2} orbital. Their σ interaction leads to a bonding, $d_\pi(\sigma_b)$, and an antibonding, $d_\pi(\sigma_{ab})$, MO. The degenerate d_π pairs are perpendicular to the M ⋯ M axis, and have the shape of the d_{xy} and $d_{x^2-y^2}$ orbitals. They undergo δ interactions that lead to a bonding degenerate $d_\pi(\delta_b)$ pair, and an antibonding degenerate $d_\pi(\delta_{ab})$ pair. The degenerate antibonding d_σ* levels, the d_{xz} and d_{yz} pairs, undergo a π interaction yielding the bonding degenerate $d_\sigma*(\pi_b)$ pair and the antibonding degenerate $d_\sigma*(\pi_{ab})$ pair. In the present systems, these levels are always empty and will therefore not be considered further.

(i) $M(OH_2)_6^{2+/3+}$ couples. In the ground state of $[Fe(OH_2)_6]_2^{5+}$, all of the 3d orbitals (Fig. 4) are singly occupied, except the $d_\pi(\sigma_b)$ one, that is doubly occupied. The electronic coupling matrix element (H_{ab}) is half of the energy for the promotion of one $d_\pi(\sigma_b)$ electron into the $d_\pi(\sigma_{ab})$ level.[1]

The ground state of $[V(OH_2)_6]_2^{5+}$ has a high-spin $d_\pi(\sigma_b)^1d_\pi(\delta_b)^2d_\pi(\delta_{ab})^2$ electron configuration, and the $d_\pi(\sigma_{ab})$ as well as all of the d_σ* levels are empty. The geometries were optimized for this state at fixed V ⋯ V distances in the range of 6.00–9.45 Å. H_{ab} is half of the energy for the $d_\pi(\sigma_b) \longrightarrow d_\pi(\sigma_{ab})$ promotion. The energies of these two states, together with H_{ab}, are reported in Table 2.

In the $[Ru(OH_2)_6]_2^{5+}$ dimer, the ground state has a (low-spin) $d_\pi(\sigma_b)^2d_\pi(\delta_b)^4d_\pi(\delta_{ab})^4d_\pi(\sigma_{ab})^1$ electron configuration (all of the d_σ* levels are empty). $1/2H_{ab}$ arises from the promotion of a $d_\pi(\sigma_b)$ electron into the $d_\pi(\sigma_{ab})$ level. This situation resembles that for the $Fe(OH_2)_6^{2+/3+}$ and the $V(OH_2)_6^{2+/3+}$ self-exchange reactions.

In the $[V(OH_2)_6]_2^{5+}$ and $[Ru(OH_2)_6]_2^{5+}$ dimers, respectively, there are 5 and 11 d_π electrons. The electron configuration of $[Ru(OH_2)_6]_2^{5+}$ can be viewed as that of $[V(OH_2)_6]_2^{5+}$ with one electron added into each d_π MO.

For the $V(OH_2)_6^{2+/3+}$ self-exchange reaction, H_{ab} increases with decreasing r in a sigmoidal manner (Fig. 5, Table 2). It is

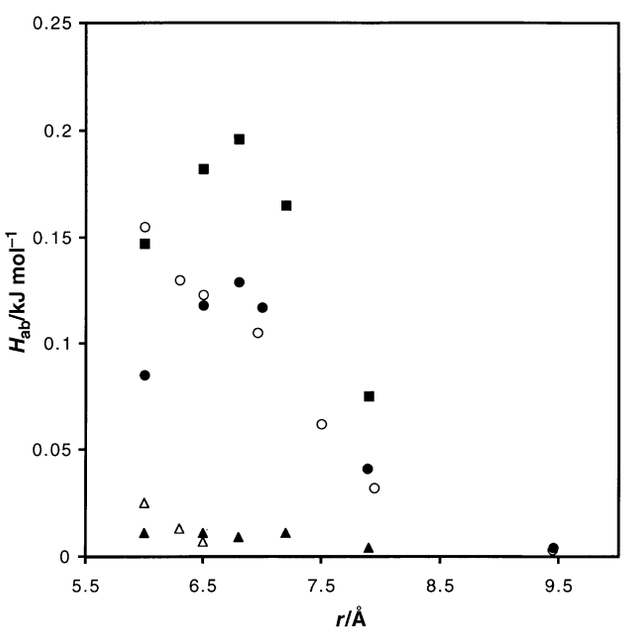

Fig. 5 Plots of the distance dependence of the electronic coupling matrix element [open circles: $V(OH_2)_6^{2+/3+}$, σ donor–acceptor interaction, open triangles: $V(OH_2)_6^{3+/4+}$, δ interaction, filled circles: $Ru(OH_2)_6^{2+/3+}$, σ interaction, filled squares: $Ru(OH_2)_6^{3+/4+}$, σ interaction, filled triangles: $Ru(OH_2)_6^{3+/4+}$, δ interaction].

worthwhile to note that the inflection point in the range of r = 6.3–6.5 Å is at the expected V ⋯ V distance of the transition state (*vide infra*). In contrast to $Fe(OH_2)_6^{2+/3+}$, the plot of ln H_{ab} *vs.* r is not linear.

For the $Ru(OH_2)_6^{2+/3+}$ self-exchange process, the distance dependence of H_{ab} differs substantially from that of $V(OH_2)_6^{2+/3+}$ and $Fe(OH_2)_6^{2+/3+}$: first, H_{ab} increases with diminishing r, reaches a maximum at ≈6.8 Å, and then decreases (Fig. 5, Table 2).

(ii) $M(OH_2)_6^{3+/4+}$ couples. In comparison with the $[V(OH_2)_6]_2^{5+}$ dimer, the electron configuration of $[V(OH_2)_6]_2^{7+}$, for which the geometry was optimized, was assumed to be $d_\pi(\sigma_b)^1 d_\pi(\delta_b)^2$, whereby all of the other levels were empty. H_{ab} was assumed to be half of the energy required for the promotion of three electrons, namely one $d_\pi(\sigma_b) \longrightarrow d_\pi(\sigma_{ab})$ promotion and two $d_\pi(\delta_b) \longrightarrow d_\pi(\delta_{ab})$ promotions whereby the latter levels are degenerate.

The MCQDPT2 calculations, however, showed that the ground state was degenerate, and that this ^4E_u state had a $d_\pi(\delta_b)^2 d_\pi(\delta_{ab})^1$ electron configuration; the $d_\pi(\sigma_b)$ and $d_\pi(\sigma_{ab})$ levels were empty. H_{ab} is thus half of the energy for the $d_\pi(\delta_b) \longrightarrow d_\pi(\delta_{ab})$ promotion (Fig. 5, Table 2). Other states, like the ^4A_g and ^4A_u ones, have higher energies (*vide infra*). H_{ab} is much smaller than for the $M(OH_2)_6^{2+/3+}$ (M = V, Fe, Ru) couples because the donor–acceptor interaction is of the δ type.

H_{ab} is considerably larger for the σ donor–acceptor interaction that, however, involves the excited ^4A_g and ^4A_u states (Table 2). The ^4A_g state, with a $d_\pi(\sigma_b)^1 d_\pi(\delta_b)^1 d_\pi(\delta_{ab})^1$ electron configuration, lies higher than the ^4E_u ground state by 37.3 kJ mol^{-1} (at a V ⋯ V distance of 6.5 Å). H_{ab} would arise form the $d_\pi(\sigma_b) \longrightarrow d_\pi(\sigma_{ab})$ promotion, but this pathway is energetically unfavorable.

The geometry of $[Ru(OH_2)_6]_2^{7+}$ was optimized for the $d_\pi(\sigma_b)^2 d_\pi(\delta_b)^4 d_\pi(\delta_{ab})^2 d_\pi(\sigma_{ab})^1$ electron configuration. The MCQDPT2 calculations showed that the ^4A_u ground state has a $d_\pi(\sigma_b)^2 d_\pi(\delta_b)^3 d_\pi(\delta_{ab})^3 d_\pi(\sigma_{ab})^1$ configuration. Obviously, the interelectronic repulsion energy is lower, when the $d_\pi(\delta_b)$ and $d_\pi(\delta_{ab})$ MOs have equal occupations. The two dominant configuration state functions (CSFs) of this state have $d_\pi(\sigma_b)^2 d_\pi(\delta_b)^4 d_\pi(\delta_{ab})^2 d_\pi(\sigma_{ab})^1$ and $d_\pi(\sigma_b)^2 d_\pi(\delta_b)^2 d_\pi(\delta_{ab})^4 d_\pi(\sigma_{ab})^1$ electron configurations. H_{ab} is sizable because it is due to a σ donor–acceptor interaction that can be described *via* a $d_\pi(\sigma_b) \longrightarrow d_\pi(\sigma_{ab})$ promotion. As for the $Ru(OH_2)_6^{2+/3+}$ couple, H_{ab} has a maximum at about 6.8 Å. Interestingly, H_{ab} for the $Ru(OH_2)_6^{3+/4+}$ couple is slightly larger than for $Ru(OH_2)_6^{2+/3+}$ (Fig. 5, Table 2).

The ^4E_u state, with a $d_\pi(\sigma_b)^1 d_\pi(\delta_b)^3 d_\pi(\delta_{ab})^4 d_\pi(\sigma_{ab})^1$ electron configuration, has a possibly insignificantly higher energy (15.4, 9.6, 7.3, 5.3, and 2.4 kJ mol^{-1}, respectively, for Ru ⋯ Ru separations of 7.9, 7.2, 6.8, 6.5, and 6.0 Å) than the ^4A_u state. For this degenerate state, H_{ab} is much smaller because it arises from a δ donor–acceptor interaction [$d_\pi(\delta_{ab}) \longrightarrow d_\pi(\delta_b)$ promotion] as in $[V(OH_2)_6]_2^{7+}$. H_{ab} for the $Ru(OH_2)_6^{3+/4+}$ self-exchange reaction *via* the δ donor–acceptor interaction (that involves the ^4E_u/^4E_g states) first increases with decreasing r, and then becomes virtually independent of r in the range of 6.0–7.2 Å (Fig. 5, Table 2).

Nuclear frequency factor (ν_n)

It was calculated according to eqns. (7) and (8).[5,7] ν_i is the average of the calculated unscaled vibrational mode i of the two reactants, for example $\nu(V^{II}–O)$ and $\nu(V^{III}–O)$, and $E_i^‡$ is the energy of this mode that is required to reach the transition state geometry. $E_i^‡$ was computed as described by Friedman and Newton.[28] The largest contributions to $\nu_{in\ +\ if}$ [eqn. (7)] arise from the high frequency modes and modes with large amplitudes. Internal coordinates that change considerably upon the electron transfer are summarized in Table 4. The M–O bond lengths and the interfacial H-bonds, $(H \cdots O)_{1-2}$, undergo large changes, whereas the O–H bonds of coordinated water, $(O–H)_1$, change much less, and the O–H bonds of water in the second coordination sphere, $(O–H)_2$, are quite insensitive to the oxidation state of the metal. The totally symmetric $(O–H)_1$ stretching mode dominates $\nu_{in\ +\ if}$ because of its high frequency [eqn. (7)]. $\nu_{in\ +\ if}$ was estimated on the basis of the M–O, $(O–H)_1$, $(H \cdots O)_{1-2}$ modes, whose frequencies are given in Table 7.

For the $M(OH_2)_6 \cdot (OH_2)_{12}^{2+}$ and $M(OH_2)_6 \cdot (OH_2)_{12}^{3+}$ ions, the assignment of the totally symmetric modes in (pseudo)-octahedral symmetry (Table 7), and the change of their corresponding internal coordinates, was straightforward. For the $M(OH_2)_6 \cdot (OH_2)_{12}^{4+}$ ions, however, totally symmetric modes in pseudo-octahedral symmetry no longer exist because of the broken H-bonds of the water trimers in the second coordination sphere (*vide infra*). This is the reason why three vibrational frequencies are reported for each mode of the $M(OH_2)_6 \cdot (OH_2)_{12}^{4+}$ ions. The average of these three modes was taken as the totally symmetric mode in pseudo-octahedral symmetry.

The frequency $\nu_{in\ +\ if}$ [eqn. (7)] is independent of r and amounts to 1219, 1275, 1901, and 2071 cm^{-1}, respectively, for the $V(OH_2)_6^{2+/3+}$, $Ru(OH_2)_6^{2+/3+}$, $V(OH_2)_6^{3+/4+}$, and $Ru(OH_2)_6^{3+/4+}$ couples. $\nu_{in\ +\ if}$ is considerably higher for the $M(OH_2)_6^{3+/4+}$ couples. ν_n [eqn. (8)] on the other hand (Table 8), depends slightly on r because of λ_{ou} that depends on r (Table 6). $\lambda_{in\ +\ if}$, being equal to $\lambda_{in} + \lambda_{if}$ and $\lambda_{fs} + \lambda_{ou}' - \lambda_{ou}$, was obtained *via* the rearrangement of eqn. (16).

For the present $M(OH_2)_6^{2+/3+}$ couples, ν_n is of the order of 800–900 cm^{-1} or (2–3) × 10^{13} s^{-1} and varies by about 10% for r = 6.0–9.5 Å (Table 8). Furthermore, ν_n is almost independent of the metal ion for a given charge of the reactants. These values are higher by a factor of about two than the frequently used values around 400 cm^{-1} that are based on the totally symmetric M–O stretching frequencies. As already mentioned, the exact value of ν_n is not needed for the computation of k because $\nu_n \gg \nu_{el}$. For the $M(OH_2)_6^{3+/4+}$ couples, ν_n is greater and in the range of 1400–1500 cm^{-1} or (4–5) × 10^{13} s^{-1}.

Second-order rate constant (k) for the self-exchange reactions

(i) $M(OH_2)_6^{2+/3+}$ couples. The nuclear frequency factor, ν_n, is much greater than the electronic frequency factor, ν_{el} (Table 8). Therefore, eqn. (5) can be approximated by the expression $\kappa_{el} = \nu_{el}/\nu_n$,[5] and the rate constant can be determined *via* eqn. (10). K_A, ν_{el}, and $\Delta E^‡$ or λ [eqn. (9)], depend on the M ⋯ M distance, r, and this data has been calculated for the $V(OH_2)_6^{2+/3+}$ and $Ru(OH_2)_6^{2+/3+}$ couples. K_A [eqns. (3) and (4)] and $\Delta E^‡$ (or λ) decrease with decreasing r. For both couples, the product of $K_A e^{-\Delta E^‡/RT}$ increases approximately by a factor of 10 with decreasing r (Table 8). For $V(OH_2)_6^{2+/3+}$, ν_{el} increases by a factor of about 25 when r decreases from ≈8 to 6.00 Å. The behavior is different for the $Ru(OH_2)_6^{2+/3+}$ couple: ν_{el} first also increases with decreasing r, then reaches a maximum at ≈6.8 Å, and finally decreases. ν_{el} follows the distance dependence of H_{ab} [eqn. (6)].

For the $V(OH_2)_6^{2+/3+}$ couple, k has a similar distance dependence as H_{ab} or ν_{el}; k increases with decreasing r. Plots of ln k *vs.* r exhibit an inflection point at about 6.5 Å as H_{ab}. For the $Fe(OH_2)_6^{2+/3+}$ couple, r was determined[1] by setting the calculated rate constant equal to the experimental value.[8] Thus, r ≈ 6.3 Å was obtained.[1] By applying the same procedure, r ≈ 7.8 Å would be estimated for the $V(OH_2)_6^{2+/3+}$ couple. This distance is too large compared with those of the $Fe(OH_2)_6^{2+/3+}$ and $Ru(OH_2)_6^{2+/3+}$ couples (*vide infra*). It will be shown in the Discussion that the experimental rate constant[9] of 0.010 M^{-1} s^{-1} (25 °C and I = 2.0 M) is too low. If it is assumed that r is in the range of 6.3–6.5 Å as for the $Fe(OH_2)_6^{2+/3+}$ and $Ru(OH_2)_6^{2+/3+}$ ions, k is estimated as 0.14–0.19 M^{-1} s^{-1} (25 °C and I = 2.0 M).

For the $Ru(OH_2)_6^{2+/3+}$ couple, the distance dependence of k is quite different: as ν_{el}, and also H_{ab}, k increases with decreasing r, reaches a maximum at ≈6.5 Å, and then decreases. The maximum is at a smaller r than for ν_{el} and H_{ab} because of the multiplication with the $K_A e^{-\Delta E^‡/RT}$ term that increases with decreasing r [eqn. (10)]. In the range of 6.0–6.8 Å, k depends only slightly on r; its maximum value of 24 M^{-1} s^{-1} (25 °C and I = 5.0 M) at r = 6.50 Å is close to the experimental value of 20 ± 4 M^{-1} s^{-1} (25 °C and I = 5.0 M).[11]

(ii) $M(OH_2)_6^{3+/4+}$ couples. For these redox couples, ν_n is larger than for the $M(OH_2)_6^{2+/3+}$ couples (M = V, Fe, Ru), while ν_{el} is

Table 7 Calculated totally symmetric vibrational frequencies[a] in the $M(OH_2)_6 \cdot (OH_2)_{12}^{n+}$ ions (M = V, Ru; n = 2, 3, 4)

	ν(M–O)/cm^{-1}	ν(H ⋯ O)$_{1-2}$/cm^{-1}	ν(O–H)$_t$/cm^{-1}
$V(OH_2)_6 \cdot (OH_2)_{12}^{2+}$	369	155	3855
$V(OH_2)_6 \cdot (OH_2)_{12}^{3+}$	537	193	3655
$V(OH_2)_6 \cdot (OH_2)_{12}^{4+}$	492, 560, 739	128, 224, 277	2243, 3204, 3543
	Average: 597	Average: 210	Average: 2997
$Ru(OH_2)_6 \cdot (OH_2)_{12}^{2+}$	401	158	3863
$Ru(OH_2)_6 \cdot (OH_2)_{12}^{3+}$	553	196	3668
$Ru(OH_2)_6 \cdot (OH_2)_{12}^{4+}$	533, 574, 716	139, 223, 282	2468, 3192, 3488
	Average: 608	Average: 215	Average: 3049

[a] The vibrational frequencies are unscaled.

Table 8 Calculated rate constants (k), and the data for its computation[a]

Redox couple	r[b]/Å	K_A/M^{-1}	λ/kJ mol^{-1}	ν_n/s^{-1}	ν_{el}/s^{-1}	κ_{el}	k/M^{-1} s^{-1}
$V^{II/III}$	9.451	0.92	269.5	2.57×10^{13}	$<3 \times 10^{7}$	$<1 \times 10^{-6}$	$<4 \times 10^{-5}$
$V^{II/III}$	7.948	0.40	254.4	2.64×10^{13}	1.12×10^{9}	4.2×10^{-5}	3.2×10^{-3}
$V^{II/III}$	7.50	0.298	248.8	2.67×10^{13}	4.26×10^{9}	1.6×10^{-4}	0.0161
$V^{II/III}$	6.959	0.199	241.0	2.71×10^{13}	1.24×10^{10}	4.6×10^{-4}	0.069
$V^{II/III}$	6.50	0.135	233.3	2.76×10^{13}	1.73×10^{10}	6.3×10^{-4}	0.141
$V^{II/III}$	6.30	0.112	229.6	2.78×10^{13}	1.95×10^{10}	7.0×10^{-4}	0.192
$V^{II/III}$	6.00	0.083	223.7	2.82×10^{13}	2.81×10^{10}	1.0×10^{-3}	0.37
$Ru^{II/III}$	9.457	1.21	223.9	2.40×10^{13}	1.87×10^{7}	7.8×10^{-7}	3.5×10^{-3}
$Ru^{II/III}$	7.888	0.56	208.1	2.49×10^{13}	2.04×10^{9}	8.2×10^{-5}	0.88
$Ru^{II/III}$	6.996	0.319	195.9	2.57×10^{13}	1.71×10^{10}	6.7×10^{-4}	14
$Ru^{II/III}$	6.80	0.278	192.8	2.59×10^{13}	2.10×10^{10}	8.1×10^{-4}	21
$Ru^{II/III}$	6.50	0.222	187.7	2.62×10^{13}	1.78×10^{10}	6.8×10^{-4}	24
$Ru^{II/III}$	6.00	0.146	178.1	2.69×10^{13}	9.47×10^{9}	3.5×10^{-4}	22
$Fe^{II/III}$[c]	6.30	0.043	203.2	2.67×10^{13}	7.4×10^{10}	2.8×10^{-3}	4
$V^{III/IV}$	6.50	0.026	273.3	4.49×10^{13}	5.19×10^{7}	1.2×10^{-6}	1.4×10^{-6}
$V^{III/IV}$	6.30	0.020	269.6	4.52×10^{13}	1.80×10^{8}	4.0×10^{-6}	5.6×10^{-6}
$V^{III/IV}$	6.00	0.013	263.7	4.57×10^{13}	6.74×10^{8}	1.5×10^{-6}	2.5×10^{-5}
$Ru^{III/IV}$	7.90	0.253	208.2	4.00×10^{13}	6.82×10^{9}[d]	1.7×10^{-4}[d]	1.31[d]
$Ru^{III/IV}$	7.90	0.253	208.2	4.00×10^{13}	1.94×10^{7}[e]	4.9×10^{-7}[e]	3.7×10^{-3}[e]
$Ru^{III/IV}$	7.20	0.142	198.9	4.09×10^{13}	3.38×10^{10}[e]	8.3×10^{-4}[d]	9.3[d]
$Ru^{III/IV}$	7.20	0.142	198.9	4.09×10^{13}	1.50×10^{8}[e]	3.7×10^{-6}[e]	0.041[e]
$Ru^{III/IV}$	6.80	0.097	192.8	4.15×10^{13}	4.84×10^{10}[d]	1.2×10^{-3}[d]	16.9[d]
$Ru^{III/IV}$	6.80	0.097	192.8	4.15×10^{13}	1.02×10^{8}[e]	2.5×10^{-6}[e]	0.036[e]
$Ru^{III/IV}$	6.50	0.071	187.7	4.21×10^{13}	4.23×10^{10}[d]	1.0×10^{-3}[d]	18.1[d]
$Ru^{III/IV}$	6.50	0.071	187.7	4.21×10^{13}	1.55×10^{8}[e]	3.7×10^{-6}[e]	0.066[e]
$Ru^{III/IV}$	6.00	0.039	178.0	4.32×10^{13}	2.83×10^{10}[d]	6.6×10^{-4}[d]	17.6[d]
$Ru^{III/IV}$	6.00	0.039	178.0	4.32×10^{13}	1.59×10^{8}[e]	3.7×10^{-6}[e]	0.099[e]

[a] $\Delta E^{\ddagger} = \lambda/4$, eqn. (9). [b] r is the M ⋯ M distance in $[M(OH_2)_6]_2^{n+}$. [c] Ref. 1. [d] σ donor–acceptor interaction ($^4A_u/^4A_g$ states). [e] δ donor–acceptor interaction ($^4E_u/^4E_g$ states).

equal or smaller (Table 8). Therefore, ν_n is much greater than ν_{el}, and k can be calculated *via* eqn. (10).

For the $V(OH_2)_6^{3+/4+}$ couple, k increases with decreasing r. Hence, the V ⋯ V separation in the transition state cannot be determined using the procedure for the $Fe(OH_2)_6^{2+/3+}$ couple, for example, because of the unavailability of experimental data. Thus, r was assumed to be similar as in the $Ru(OH_2)_6^{2+/3+}$, $Ru(OH_2)_6^{3+/4+}$, and $Fe(OH_2)_6^{2+/3+}$ couples, and k for the $V(OH_2)_6^{3+/4+}$ self-exchange reaction is estimated as (1–6) × 10^{-6} M^{-1} s^{-1} for r = 6.3–6.5 Å (25 °C, I = 2.0 M).

For the $Ru(OH_2)_6^{3+/4+}$ couple, two cases have to be considered because the present $[M(OH_2)_6]_2^{n+}$ model, in which hydration had to be neglected, is possibly not adequate for the determination of the energy difference between the ^4A_u and the ^4E_u states (Table 2). If the energy of the ^4E_u state is considerably lower than that of the ^4A_u state, the electron transfer would proceed *via* a δ donor–acceptor interaction. The calculated rate constant first increases with decreasing r, and then levels off as H_{ab} (Table 8). Assuming that the Ru ⋯ Ru distance in the transition state is ≈6.5 Å, $k \approx 0.07$ M^{-1} s^{-1} (25 °C, I = 5.0 M) is estimated. If the energy of the ^4E_u state is equal to or higher than that of the ^4A_u state, the electron transfer would proceed *via* the σ donor–acceptor interaction. In this case, k has a maximum at $r \approx 6.5$ Å, at which it is equal to 18 M^{-1} s^{-1} (25 °C and I = 5.0 M).

Discussion

For the $Fe(OH_2)_6^{2+/3+}$ couple, the calculated rate constant decreased with increasing r. The Fe ⋯ Fe distance in the transition state was determined by comparing the calculated[1] second-order rate constant (k) with the experimental[8] value. Thus, $r \approx 6.3$ Å was found.

The distance dependence of k for the $Ru(OH_2)_6^{2+/3+}$ couple is different: k is maximal at $r \approx 6.5$ Å. Interestingly, at this distance, the calculated value agrees with the experimental[11] one. Thus, it may be concluded that the Ru ⋯ Ru separation in the transition state is ≈6.5 Å. This distance agrees with the slightly smaller one for the $Fe(OH_2)_6^{2+/3+}$ couple whose ionic radii are smaller. The electron transfer takes place with the reactants in approximately closest contact.

As already mentioned in the Results section, the application

of this procedure for the determination of r to the $V(OH_2)_6^{2+/3+}$ self-exchange reaction yields a V ⋯ V separation of ≈7.8 Å. The fact that, on one hand, this value is considerably larger than those for the $Fe(OH_2)_6^{2+/3+}$ and $Ru(OH_2)_6^{2+/3+}$ couples, and that, on the other hand, the ionic radii of the $V(OH_2)_6^{2+}$ and $V(OH_2)_6^{3+}$ ions lie between those of the corresponding hexaaqua ions of Fe and Ru, indicates that the experimental[9] value of 0.010 M^{-1} s^{-1} (25 °C and I = 2.0 M) is too low. A critical analysis of the experimental details[9] shows that this is indeed the case: the reaction has been investigated in perchlorate medium. It is known[12] that $V(OH_2)_6^{2+}$ reacts quite rapidly with ClO_4^-. Thus, ClO_4^- and the products of this side reaction as well (*e.g.* VO^{2+}, $ClO_3^{\bullet}$, ClO_3^-, ...) reacted with $V(OH_2)_6^{2+}$ and thus removed tagged $V(OH_2)_6^{2+}$ that had been formed *via* the self-exchange reaction. Therefore, the formation of tagged $V(OH_2)_6^{2+}$ occurred more slowly, and the observed rate constant is too low. If it is assumed that the V ⋯ V distance is similar as in the other two $M(OH_2)_6^{2+/3+}$ (M = V, Ru) couples, r = 6.3–6.5 Å is estimated. The rate constant for the $V(OH_2)_6^{2+/3+}$ self-exchange reaction would then be in the range of 0.14–0.19 M^{-1} s^{-1} (25 °C and I = 2.0 M).

The electron self-exchange reactions involving the di- and tri-valent first row transition metal hexaaqua ions have been investigated recently by Rosso and Rustad[29] using density functional theory (DFT). Their calculations of λ were based on a smaller model involving the $M(OH_2)_6^{2+/3+}$ ions without second coordination spheres. Therefore, they did not include the interfacial reorganizational energy (λ_{if}). Their approach for the computation of k was quite different and involved parameters that were obtained *via* a fit to experimental data. In particular, H_{ab} was not calculated quantum chemically. Nevertheless, with their combination of computed and experimental data, they estimated the $V(OH_2)_6^{2+/3+}$ self-exchange rate as 0.30 M^{-1} s^{-1}. This value is close to that suggested by the present investigation.

The calculated rate constant for the $V(OH_2)_6^{2+/3+}$ self-exchange reaction increases with decreasing r. This raises the question, why the reaction does not take place at V ⋯ V distances smaller than ≈6.3–6.5 Å. The increase of k with decreasing r, that was also found[1] for the $Fe(OH_2)_6^{2+/3+}$ couple, is an artifact arising from the limitation of the model: it should be recalled that the λ_{fs} component of the reorganizational energy was calculated on the basis of *free* $V(OH_2)_6{\cdot}(OH_2)_{12}^{2+}$ and $V(OH_2)_6{\cdot}(OH_2)_{12}^{3+}$ ions. When these reactants (including their quite strongly bound second coordination spheres) are brought closer together than about 6.3 Å, interfacial $(H \cdots O)_{1-2}$ bonds are likely to be strained substantially or perhaps even broken. The energy arising from these processes would have to be added to the Coulomb repulsion energy (w_r), and K_A [eqn. (3)] would diminish sharply. At small r, the constant for the association of the reactants, K_A, no longer can be estimated *via* eqns. (3) and (4); K_A would be smaller. Classical molecular dynamics (MD) simulations on the $Fe(OH_2)_6^{2+/3+}$ electron self-exchange reaction yielded an Fe ⋯ Fe separation of 5.5 Å in the transition state.[30,31] Although MD simulations are subject to different approximations than the present quantum chemical study, they show that there is an optimum distance for the electron transfer.

The second-order rate constant for the $V(OH_2)_6^{3+/4+}$ self-exchange reaction had to be estimated at the likely V ⋯ V separation of 6.3–6.5 Å. k is very small, (1–6) × 10^{-6} M^{-1} s^{-1} (25 °C and I = 2.0 M), for two reasons: first, the reorganizational energy is high (Table 3) and second, the electronic coupling matrix element is small (Table 2). The small H_{ab} arises from the δ donor–acceptor interaction.

k for the $Ru(OH_2)_6^{3+/4+}$ self-exchange reaction proceeding *via* a δ donor–acceptor interaction is equal to ≈0.07 M^{-1} s^{-1} (25 °C and I = 5.0 M) at the likely Ru ⋯ Ru separation of about 6.5 Å. For the σ donor–acceptor interaction, k is maximal at r ≈ 6.5 Å, as for the $Ru(OH_2)_6^{2+/3+}$ self-exchange process and estimated as ≈18 M^{-1} s^{-1} (25 °C and I = 5.0 M). Interestingly, this value is virtually the same as that for the $Ru(OH_2)_6^{2+/3+}$ self-exchange reaction. At the first glance, this might appear unlikely, but it should be noted that these two ruthenium couples have equal reorganizational energies (Table 3). Furthermore, in both redox systems, the electron transfer proceeds *via* the (strong) σ donor–acceptor interaction. Nevertheless, it is not yet established whether the σ pathway is favored energetically over the δ one. It should be noted that the computed λ of the $M(OH_2)_6^{3+/4+}$ couples are less accurate than those of $M(OH_2)_6^{2+/3+}$. In the $M(OH_2)_6^{4+}$ ions, the third coordination sphere might be bound more strongly to the second one because of their high charge. Possibly, a second λ_{if} term, describing the reorganizational energy of the H-bonds between the second and third coordination spheres, should be included. Thus, the present reorganizational energies might be too low.

In all of the presently investigated redox couples, and the $Fe(OH_2)_6^{2+/3+}$ couple as well, a nonbonding electron is exchanged. The electron self-exchange rates (k) depend on the metal and its oxidation states. The charge of the reactants, the temperature, and the ionic strength affect K_A. The first-order rate constant for the electron transfer step, k_{el}, which is defined as k/K_A, is equal to $\nu_{el}e^{-\Delta E^{\ddagger}/RT}$ (for $\nu_n \gg k_{el}$). k_{el} is independent of the charge of the reactants and the medium (*e.g.* the ionic strength). It is approximately equal for the $Fe(OH_2)_6^{2+/3+}$ and $Ru(OH_2)_6^{2+/3+}$ couples (≈90 s^{-1}), although their respective reorganizational energies (λ) and electronic frequency factors (ν_{el}) are different (Table 8). The higher λ for $Fe(OH_2)_6^{2+/3+}$, which would give rise to a lower k_{el}, is counterbalanced by the higher ν_{el} value. ν_{el} is different (by a factor of about 4) for the above two redox couples in spite of their similar donor–acceptor interactions that are of the σ type: in both cases H_{ab} is due to a $d_\pi(\sigma_b) \longrightarrow d_\pi(\sigma_{ab})$ promotion [see "Electronic coupling matrix element (H_{ab})" section].

For the $V(OH_2)_6^{2+/3+}$ couple, k_{el} is much smaller and in the range of 1.0–1.7 s^{-1}. This low k_{el} is due to the relatively high reorganizational energy; ν_{el} is only slightly smaller than for $Ru(OH_2)_6^{2+/3+}$. It is interesting to note that for the present three self-exchange reactions, in which a nonbonding electron is exchanged, λ as well as ν_{el} are different. The variation in λ arises from the different λ_{fs} (Table 3), that are composed by λ_{in} and λ_{if}. λ_{ou} and λ_{ou}', that depend on r and the ionic radii, are virtually equal for all of the presently discussed couples.

For the $V(OH_2)_6^{3+/4+}$ self-exchange reaction, k_{el} is very small and in the range of 6 × 10^{-5}–3 × 10^{-4} s^{-1}. In contrast, the corresponding $Ru(OH_2)_6^{3+/4+}$ reaction is much faster: k_{el} is equal to 0.9 and 250 s^{-1}, respectively, for the δ and σ donor–acceptor interactions, whereby, as already mentioned, the pathway is unknown.

The interfacial reorganizational energy, λ_{if} (Table 3), is in the range of 17–28 kJ mol^{-1} for the present $M(OH_2)_6^{2+/3+}$ couples, and makes a non negligible contribution of about 4–7 kJ mol^{-1} to $\Delta E^{\ddagger}$. For the $M(OH_2)_6^{3+/4+}$ (M = V, Ru) couples, λ_{if} is much larger, 54–80 kJ mol^{-1}, and comparable to or even larger than the inner shell reorganizational energy, λ_{in}. The large reorganizational energy of $V(OH_2)_6^{3+/4+}$ is due to λ_{if}; λ_{in} is even smaller than for $V(OH_2)_6^{2+/3+}$. The reorganizational energies of $Ru(OH_2)_6^{2+/3+}$ and $Ru(OH_2)_6^{3+/4+}$ are equal, whereby the larger λ_{if} term of $Ru(OH_2)_6^{3+/4+}$ is compensated by the smaller λ_{in} component. Because, in the $M(OH_2)_6^{3+/4+}$ couples, the second coordination sphere is bound strongly to the first one, the values of the λ_{in} and λ_{if} components may be only approximate, but λ_{fs} is an accurate energy.

The rates of cross reactions can be predicted *via* the Marcus cross-relation.[32] It is based on the assumption that eqn. (19) holds.

$$\nu_{el,AB} \approx (\nu_{el,AA}\nu_{el,BB})^{1/2} \qquad (19)$$

If the self-exchange and cross reactions involve similar geometries of the transition states and the same donor–acceptor interaction, eqn. (19) is likely to be approximately valid. How-

ever, if, for example, the self-exchange reactions within redox couples A and B proceed *via* σ and δ interactions and a face-to-face approach, $v_{el,AB}$ for the cross reaction is unlikely to be predictable *via* eqn. (19). $v_{el,AB}$ depends on the geometry and the electronic interaction in the transition state $[AB]^{\ddagger}$. The A and B reactants can approach in a face-to-face, edge-to-edge, apex-to-apex, face-to-apex, edge-to-apex or face-to-edge arrangement, in which σ, π or δ donor–acceptor interactions are possible. The A ⋯ B separation is shortest for the face-to-face and longest for the apex-to-apex approach. The experimental determination[33] of the self-exchange rate of the $Mn(OH_2)_6^{2+/3+}$ couple is such a striking example: $k(Mn^{2+/3+})$ obtained *via* cross reactions with $ML_3^{2+/3+}$ (M = Fe, Ru, Os, L = polypyridyl or phenanthroline ligands), $Fe(OH_2)_6^{2+/3+}$, $Ni(cyclam)^{2+/3+}$, $Ni(H_2oxime)^{2+/3+}$, and $Co(OH_2)_6^{2+/3+}$ was 10^{-9}, 3×10^{-6}, 10^{-5}, 6×10^{-4}, and 4×10^{-3} M^{-1} s^{-1}; $k(Mn^{2+/3+})$ varies by a factor of 4×10^6.

Summary

The second-order rate constants (k) for the electron self-exchange reactions *via* the outer-sphere pathway were computed on the basis of the equation $k = K_A v_{el} e^{-\Delta E^{\ddagger}/RT}$, that is valid because $v_n \gg v_{el}$. For all of the presently investigated hexaaqua ions, and the $Fe(OH_2)_6^{2+/3+}$ couple[1] as well, the reorganizational energy of the H-bonds between the first and second coordination spheres (λ_{if}) is sizable [17–28 and 54–80 kJ mol^{-1}, respectively, for $M(OH_2)_6^{2+/3+}$ and $M(OH_2)_6^{3+/4+}$ couples]. Even for the exchange of a nonbonding electron having a σ donor–acceptor interaction, as in the case of the $M(OH_2)_6^{2+/3+}$ (M = V, Fe, Ru) couples, v_{el} varies. This suggests that the reorganizational energies (λ) cannot be obtained in a straightforward manner from kinetic data. In the widely used expression like, for example, $k = Ze^{-\Delta E^{\ddagger}/RT}$, the collision frequency factor Z is not a constant, even if variations of the charge of the reactants and the ionic strength are taken into account. v_{el} is sensitive to the nature (σ, π or δ) of the donor–acceptor interaction; striking examples are the different H_{ab} values for δ and σ interactions of the $M(OH_2)_6^{3+/4+}$ couples. Even for equal donor–acceptor interactions, as in the $Fe(OH_2)_6^{2+/3+}$ and $Ru(OH_2)_6^{2+/3+}$ self-exchange reactions, v_{el} can vary substantially. Failures of the Marcus cross-relation[32] might arise from the non-applicability of the implicitly included relation $v_{el,AB} \approx v_{el,AA} v_{el,BB})^{1/2}$.

References

1 F. P. Rotzinger, submitted for publication.
2 R. A. Marcus, *Annu. Rev. Phys. Chem.*, 1964, **15**, 155.
3 N. S. Hush, *Trans. Faraday Soc.*, 1961, **57**, 557.
4 V. G. Levich, R. R. Dogonadze and A. M. Kuznetsov, *Electrochim. Acta*, 1968, **13**, 1025.
5 N. Sutin, *Prog. Inorg. Chem.*, 1983, **30**, 441.
6 R. M. Fuoss, *J. Am. Chem. Soc.*, 1958, **80**, 5059.
7 M. D. Newton and N. Sutin, *Annu. Rev. Phys. Chem.*, 1984, **35**, 437.
8 J. Silverman and R. W. Dodson, *J. Phys. Chem.*, 1952, **56**, 846.
9 K. V. Krishnamurty and A. C. Wahl, *J. Am. Chem. Soc.*, 1958, **80**, 5921.
10 W. Böttcher, G. M. Brown and N. Sutin, *Inorg. Chem.*, 1979, **18**, 1447.
11 P. Bernhard, L. Helm, A. Ludi and A. E. Merbach, *J. Am. Chem. Soc.*, 1985, **107**, 312.
12 Y. Ducommun, D. Zbinden and A. E. Merbach, *Helv. Chim. Acta*, 1982, **65**, 1385.
13 M. W. Schmidt, K. K. Baldridge, J. A. Boatz, S. T. Elbert, M. S. Gordon, J. H. Jensen, S. Koseki, N. Matsunaga, K. A. Nguyen, S. J. Su, T. L. Windus, M. Dupuis and J. A. Montgomery, *J. Comput. Chem.*, 1993, **14**, 1347.
14 W. J. Stevens, M. Krauss, H. Basch and P. G. Jasien, *Can. J. Chem.*, 1992, **70**, 612.
15 W. J. Hehre, R. Ditchfield and J. A. Pople, *J. Chem. Phys.*, 1972, **56**, 2257.
16 R. Ditchfield, W. J. Hehre and J. A. Pople, *J. Chem. Phys.*, 1971, **54**, 724.
17 W. J. Hehre, R. F. Stewart and J. A. Pople, *J. Chem. Phys.*, 1969, **51**, 2657.
18 F. A. Cotton, L. M. Daniels, C. A. Murillo and J. F. Quesada, *Inorg. Chem.*, 1993, **32**, 4861.
19 J. K. Beattie, S. P. Best, B. W. Skelton and A. H. White, *J. Chem. Soc., Dalton Trans.*, 1981, 2105.
20 P. Bernhard, H.-B. Bürgi, J. Hauser, H. Lehmann and A. Ludi, *Inorg. Chem.*, 1982, **21**, 3936.
21 S. Miertus, E. Scrocco and J. Tomasi, *Chem. Phys.*, 1981, **55**, 117.
22 J. Tomasi and M. Persico, *Chem. Rev.*, 1994, **94**, 2027.
23 J. Tomasi and R. Cammi, *J. Comput. Chem.*, 1995, **16**, 1449.
24 H. Nakano, *J. Chem. Phys.*, 1993, **99**, 7983.
25 K. Hirao, *Chem. Phys. Lett.*, 1992, **190**, 374.
26 F. P. Rotzinger, *J. Phys. Chem. A*, 1999, **103**, 9345.
27 Y.-K. Choe, Y. Nakao and K. Hirao, *J. Chem. Phys.*, 2001, **115**, 621.
28 H. L. Friedman and M. D. Newton, *J. Electroanal. Chem.*, 1986, **204**, 21.
29 K. M. Rosso and J. R. Rustad, *J. Phys. Chem. A*, 2000, **104**, 6718.
30 R. A. Kuharski, J. S. Bader, D. Chandler, M. Sprik, M. L. Klein and R. W. Impey, *J. Chem. Phys.*, 1988, **89**, 3248.
31 J. S. Bader and D. Chandler, *J. Phys. Chem.*, 1992, **96**, 6423.
32 R. A. Marcus, *Discuss. Faraday Soc.*, 1960, **29**, 21, 129.
33 D. H. Macartney and N. Sutin, *Inorg. Chem.*, 1985, **24**, 3403.